Mineralogical Magazine, October 2018, Vol. 82(5), pp. 1089–1100

Markeyite, a new calcium uranyl carbonate mineral from the Markey mine, San Juan County, Utah, USA

ANTHONY R. KAMPF[1,*], JAKUB PLÁŠIL[2], ANATOLY V. KASATKIN[3], JOE MARTY[4] AND JIŘÍ ČEJKA[5]

[1] Mineral Sciences Department, Natural History Museum of Los Angeles County, 900 Exposition Boulevard, Los Angeles, CA 90007, USA
[2] Institute of Physics ASCR, v.v.i., Na Slovance 1999/2, 18221 Prague 8, Czech Republic
[3] Fersman Mineralogical Museum of the Russian Academy of Sciences, Leninsky Prospekt, 18-2, 119071, Moscow, Russia
[4] 5199 East Silver Oak Road, Salt Lake City, UT 84108, USA
[5] Department of Mineralogy and Petrology, National Museum, Cirkusová 1740, 193 00, Prague 9, Czech Republic

[*Received 3 July 2017; Accepted 19 October 2017; Associate Editor: Ian Graham*]

ABSTRACT

The new mineral markeyite (IMA2016-090), $Ca_9(UO_2)_4(CO_3)_{13}\cdot 28H_2O$, was found in the Markey mine, San Juan County, Utah, USA, where it occurs as a secondary phase on asphaltum in association with calcite, gypsum and natrozippeite. The mineral is pale yellowish-green with white streak and fluoresces bright bluish white under a 405 nm laser. Crystals are transparent and have vitreous to pearly lustre. It is brittle, with Mohs hardness 1½ to 2, irregular fracture and three cleavages: perfect on {001}; good on {100} and {010}. The measured density is 2.68 g cm^{-3}. Crystals are blades, flattened on {001} and elongate on [010], exhibiting the forms {100}, {010}, {001}, {110}, {101}, {011} and {111}. Markeyite is optically biaxial (–) with $\alpha = 1.538(2)$, $\beta = 1.542(2)$ and $\gamma = 1.545(2)$ (white light); the measured 2V is 81(2)°; the dispersion is $r < v$ (weak); the optical orientation is $X = \mathbf{c}$, $Y = \mathbf{b}$, $Z = \mathbf{a}$; and pleochroism is X = light greenish yellow, Y and Z = light yellow ($X > Y \approx Z$). Electron microprobe analyses (energy-dispersive spectroscopy mode) yielded CaO 18.60, UO_3 42.90, CO_2 21.30 (calc.) and H_2O 18.78 (calc.), total 101.58 wt.% and the empirical formula $Ca_{8.91}(U_{1.01}O_2)_4(CO_3)_{13}\cdot 28H_2O$. The six strongest powder X-ray diffraction lines are [d_{obs} Å(I)(hkl)]: 10.12(69)(001), 6.41(91)(220,121), 5.43(100)(221), 5.07(33)(301,002,131), 4.104(37)(401,141) and 3.984(34)(222). Markeyite is orthorhombic, *Pmmn*, $a = 17.9688(13)$, $b = 18.4705(6)$, $c = 10.1136(4)$ Å, $V = 3356.6(3)$ Å^3 and $Z = 2$. The structure of markeyite ($R_1 = 0.0435$ for 3427 $F_o > 4\sigma F$) contains uranyl tricarbonate clusters (UTC) that are linked by Ca–O polyhedra forming thick corrugated heteropolyhedral layers. Included within the layers is an additional disordered CO_3 group linking the Ca–O polyhedra. The layers are linked to one another and to interlayer H_2O groups only via hydrogen bonds. The structure bears some similarities to that of liebigite.

KEYWORDS: markeyite, new mineral, uranyl tricarbonate, crystal structure, liebigite, Markey mine, Utah, USA.

Introduction

IN recent years, mines in the Red Canyon portion of the White Canyon district in south-eastern Utah have yielded many new minerals. Our investigation of the secondary mineralization at the Blue Lizard mine has already resulted in the description of sixteen new minerals, most of which are Na uranyl sulfates. As we have expanded our efforts to other nearby uranium mines in Red Canyon, additional new species are being revealed. The new Na–Mg uranyl carbonate leószilárdite (Olds *et al.*, 2016) was recently described from the Markey mine and, herein, we describe another new uranyl carbonate, markeyite, from this mine.

*E-mail: akampf@nhm.org
https://doi.org/10.1180/minmag.2017.081.085

Markeyite (/ma:r 'ki: ait/) is named for the locality, the Markey mine. The new mineral and name were approved by the International Mineralogical Association Commission on New Minerals, Nomenclature and Classification (IMA 2016-090). After the initial approval of the mineral and its publication in the CNMNC Newsletter No. 35 (Kampf *et al*., 2017), a change in the formula from $Ca_9(UO_2)_4(CO_3)_{12}(OH)_2{\cdot}28H_2O$ to $Ca_9(UO_2)_4(CO_3)_{13}{\cdot}28H_2O$ was approved by the officers of the CNMNC (Hålenius *et al*., 2017). The description is based on one holotype and five cotype specimens. The holotype and four cotypes are deposited in the collections of the Natural History Museum of Los Angeles County, 900 Exposition Boulevard, Los Angeles, CA 90007, USA, catalogue numbers 67091 (holotype), 67092, 67093, 67094 and 69095, respectively. One cotype specimen is housed in the collections of the Fersman Mineralogical Museum of the Russian Academy of Sciences, Moscow, Russia, with registration number 4932/1.

Occurrence

Markeyite was found underground in the Markey mine, Red Canyon, White Canyon District, San Juan County, Utah, USA (37°32′57″N, 110°18′08″W). The Markey mine is located ~1 km southwest of the Blue Lizard mine, on the east-facing side of Red Canyon, ~72 km west of the town of Blanding, Utah, and ~22 km southeast of Good Hope Bay on Lake Powell. The geology of the Markey Mine is quite similar to that of the Blue Lizard mine (Chenoweth, 1993; Kampf *et al*., 2016), although the secondary mineralogy of the Markey mine is notably richer in carbonate phases. The information following is taken largely from Chenoweth (1993).

Jim Rigg of Grand Junction, Colorado began staking claims in Red Canyon in March of 1949. The Markey group of claims, staked by Rigg and others, was purchased by the Anaconda Copper Mining Company on June 1, 1951. After limited exploration and production, the mine closed in 1955. The mine was subsequently acquired from Anaconda by Calvin Black of Blanding, Utah under whose ownership the mine operated from 1960 to 1982 and was a leading producer in the district for nearly that entire period.

The uranium deposits in Red Canyon occur within the Shinarump member of the Upper Triassic Chinle Formation, in channels incised into the reddish-brown siltstones of the underlying Lower Triassic Moenkopi Formation. The Shinarump member consists of medium- to coarse-grained sandstone, conglomeratic sandstone beds and thick siltstone lenses. Ore minerals were deposited as replacements of wood and other organic material and as disseminations in the enclosing sandstone. Since the mine closed in 1982, oxidation of primary ores in the humid underground environment has produced a variety of secondary minerals, mainly carbonates and sulfates, as efflorescent crusts on the surfaces of mine walls.

Markeyite is a rare mineral in the secondary mineral assemblage. It occurs on asphaltum in association with calcite, gypsum and natrozippeite. Other secondary minerals in the general assemblage include: ammoniozippeite, andersonite, anglesite, aragonite, arsenuranospathite, atacamaite, bayleyite, bluelizardite, bobcookite, brochantite, čejkaite, chalcanthite, chalconatronite, chinleite-(Y), covellite, cuprosklodowskite, cyanotrichite, deliensite, devilline, erythrite, eugsterite, fermiite, jarosite, johannite, klaprothite, leószilárdite, leydetite, magnesioleydetite, mahnertite, malachite, marécottite, melanterite, metakahlerite, metasideronatrite, natrojarosite, plášilite, posnjakite, pseudojohannite, redcanyonite, römerite, sabugalite, schröckingerite, sideronatrite, sulfur, thénardite, thérèsemagnanite, uramarsite, uranospathite, wetherillite, zippeite and other potentially new minerals currently under investigation.

Physical and optical properties

Markeyite crystals are blades and tablets (Fig. 1) up to ~1 mm in maximum dimension, flattened on {001} and elongate on [010]. Measurements on a Huber Reflection Goniometer 302 confirmed the crystal forms {100}, {010}, {001}, {110}, {101}, {011} and {111} (Fig. 2). No twinning was observed.

Crystals are pale yellowish green and transparent with vitreous lustre. The streak is white. The mineral fluoresces bright bluish white under a 405 nm laser. The Mohs hardness is between 1½ and 2, based upon scratch tests. Crystals are brittle with irregular fracture and three cleavages: perfect on {001}, good on {100} and {010}. At room temperature, the mineral dissolves very slowly in H_2O (minutes) and dissolves immediately with effervescence in dilute HCl. The density measured by flotation in a mixture of methylene iodide and

https://doi.org/10.1180/minmag.2017.081.085 Published online by Cambridge University Press

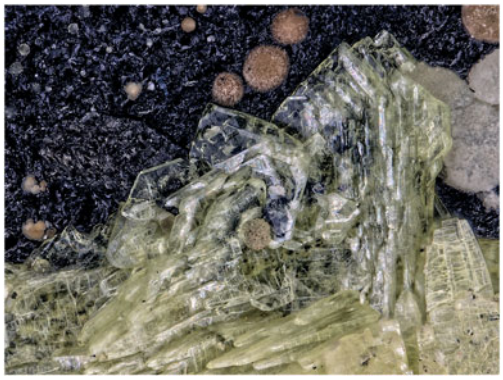

FIG. 1. Markeyite (blades in centre) with similar new Ca uranyl carbonate (tapering crystals along bottom) and calcite (brown and grey balls) on asphaltum; field of view: 1.6 mm across.

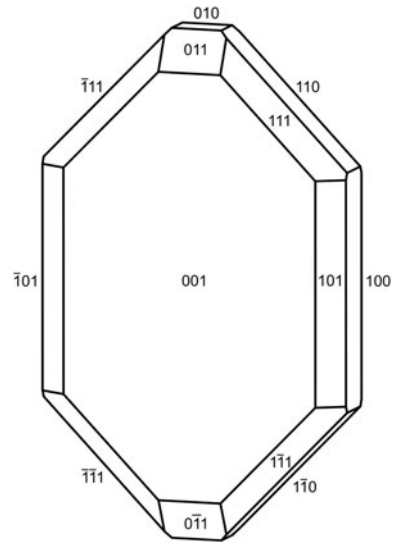

FIG. 2. Crystal drawing of markeyite; clinographic projection in nonstandard orientation, [010] vertical.

toluene is 2.68(2) g/cm^3. The calculated density based on the empirical formula and unit-cell parameters obtained from single-crystal X-ray diffraction data is 2.699 g/cm^3.

Optically, markeyite is biaxial (–), with $\alpha =$ 1.538(1), $\beta = 1.542(1)$ and $\gamma = 1.545(1)$ (measured in white light). The 2V measured directly on a spindle-stage is 81(2)°; the calculated 2V is 81.6°. Dispersion is $r < v$, weak. The mineral is weakly pleochroic: $X =$ light greenish yellow, $Y \approx Z =$ light yellow; $X > Y \approx Z$. The optical orientation is $X =$ **c**, $Y =$ **b**, $Z =$ **a**.

Raman spectroscopy

Raman spectroscopy was conducted on a Horiba XploRA PLUS using a 532 nm diode laser. A background correction was applied using the Horiba software. The Raman spectrum of markeyite is shown in Fig. 3.

The broad multiple bands in the 3700–3300 and 2800–2300 cm^{-1} ranges are attributed to ν O–H stretching vibrations of structurally nonequivalent/symmetrically distinct hydrogen-bonded OH and H_2O groups. The 3700–3300 cm^{-1} range corresponds to weak hydrogen bonds and the 2800–2300 cm^{-1} range to strong hydrogen bonds (Libowitzky, 1999). A weak, broad band centred at ~1600 cm^{-1} is attributed to the ν_2 (δ) bending vibrations of H_2O.

The aforementioned H_2O band partly overlaps with a very weak broad band associated with the split doubly degenerate ν_3 $(CO_3)^{2-}$ antisymmetric stretching vibrations of the $(CO_3)^{2-}$ units, with a more distinct weak band at 1412 cm^{-1}. Medium to strong bands at 1095, 1086, 1078 and 1067 cm^{-1} are connected with the ν_1 $(CO_3)^{2-}$ symmetric stretching vibrations. These bands are consistent with the presence of four structurally nonequivalent carbonate units (Koglin *et al*., 1979; Anderson *et al*., 1980; Čejka, 1999 and 2005; and references therein), but do not preclude the presence of a fifth carbonate unit.

A weak band at 882 cm^{-1} may be due to the ν_2 (δ) $(CO_3)^{2-}$ bending vibrations or to the ν_3 $(UO_2)^{2+}$ antisymmetric stretching vibration corresponding with the U–O bond length in uranyl at ~1.80 Å; an overlap/coincidence of these two bands is possible. A very strong band at 825 cm^{-1} is assigned to the ν_1 $(UO_2)^{2+}$ symmetric stretching vibrations and provides an inferred U–O bond length of ~1.79 Å (Bartlett and Cooney, 1989). Also a coincidence of the ν_2 (δ) $(CO_3)^{2-}$ bending vibration and ν_1 $(UO_2)^{2+}$ symmetric stretching vibration is likely.

Weak to strong bands at 772, 751, 733 and 694 cm^{-1} are assigned to the doubly degenerate ν_4 (δ) $(CO_3)^{2-}$ bending vibrations. A medium broad band at 238 cm^{-1} is assigned to the split doubly degenerate ν_2 (δ) $(UO_2)^{2+}$ bending vibrations and weak to medium bands at 170, 155 and 128 cm^{-1} to the lattice modes (Koglin *et al*., 1979; Anderson *et al*., 1980; Čejka, 1999 and 2005).

https://doi.org/10.1180/minmag.2017.081.085 Published online by Cambridge University Press

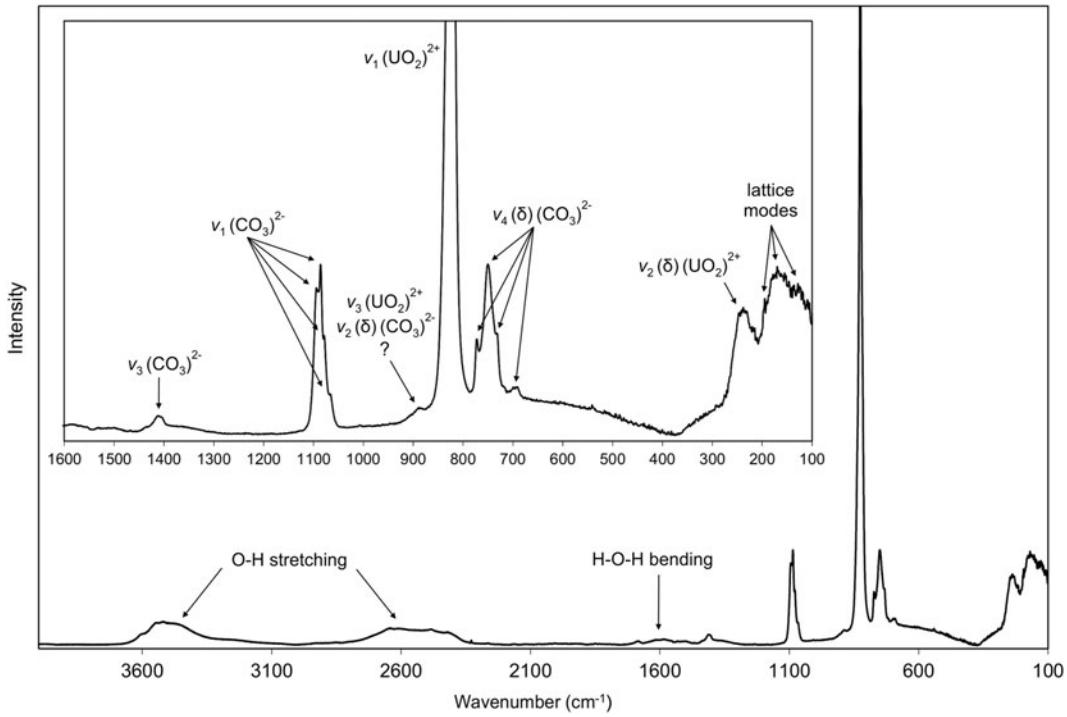

FIG. 3. The Raman spectrum of markeyite.

Chemical composition

Chemical analyses (nine) were performed using a CamScan 4D electron microprobe in energy-dispersive spectroscopy mode (20 kV, 5 nA and 3 μm beam diameter). Attempts to use wavelength-dispersive spectroscopy with a higher beam current were made, but resulted in partial dehydration and totals significantly higher than 100 wt.%. H_2O and CO_2 were not determined directly because of extreme paucity of material. The H_2O and CO_2 contents were calculated by stoichiometry on the basis of 75 O atoms per formula unit and confirmed by the crystal-structure refinement and Raman spectroscopy. No other elements with atomic numbers higher than 8 were observed. Analytical data are given in Table 1.

The empirical formula is $Ca_{8.91}(U_{1.01}O_2)_4(CO_3)_{13}{\cdot}28H_2O$. The ideal formula is $Ca_9(UO_2)_4(CO_3)_{13}{\cdot}28H_2O$ which requires CaO 18.52, UO_3 41.98, CO_2 20.99 and H_2O 18.51, total 100 wt.%. The Gladstone-Dale compatibility index $1 - (K_P/K_C)$ for the empirical formula is –0.027, in the excellent range (Mandarino, 2007), using $k(UO_3) = 0.118$, as provided by Mandarino (1976).

X-ray crystallography and structure refinement

Powder X-ray studies were done using a Rigaku R-Axis Rapid II curved imaging plate micro-diffractometer, with monochromatized Mo$K\alpha$ radiation ($\lambda = 0.71075$ Å). A Gandolfi-like motion on the ϕ and ω axes was used to randomize the sample and observed d values and intensities

TABLE 1. Chemical composition (in wt.%) for markeyite.

Constituent	Mean	Range	S.D.	Standard
CaO	18.60	17.87–19.34	0.52	wollastonite
UO_3	42.90	41.10–44.60	1.07	syn. UO_2
CO_2*	21.30			
H_2O*	18.78			
Total	101.58			

* Based on the structure.
S.D. – Standard deviation.

https://doi.org/10.1180/minmag.2017.081.085 Published online by Cambridge University Press

were derived by profile fitting using *JADE 2010* software (Materials Data, Inc.). The powder data presented in Table 2 show good agreement with the pattern calculated from the structure determination. Unit-cell parameters refined from the powder data using JADE 2010 with whole pattern fitting are: $a = 17.9688(13)$, $b = 18.4705(6)$, $c = 10.1136(4)$ Å and $V = 3356.6(3)$ Å^3.

The single-crystal structure data were collected at room temperature using the same diffractometer

TABLE 2. Powder X-ray diffraction data (d in Å) for markeyite. Only calculated lines with $I \geq 2$ are listed.

I_{obs}	d_{obs}	d_{calc}	I_{calc}	hkl	I_{obs}	d_{obs}	d_{calc}	I_{calc}	hkl	I_{obs}	d_{obs}	d_{calc}	I_{calc}	hkl
69	10.12	10.1136	100	0 0 1			2.9450	3	0 6 1			2.0656	2	8 3 1
		9.2353	2	0 2 0			2.9378	6	3 0 3			2.0550	3	5 1 4
13	8.77	8.9844	3	2 0 0	22	2.921	2.9122	5	2 6 0	21	2.0518	2.0468	2	5 5 3
6	8.11	7.9543	3	1 1 1			2.9062	4	1 6 1			2.0451	3	2 8 2
		6.7168	3	2 0 1			2.9014	2	3 1 3			2.0423	3	7 0 3
91	6.41	6.4398	42	2 2 0			2.8932	2	5 1 2			2.0299	3	7 1 3
		6.3760	16	1 2 1	7	2.876	2.8715	3	6 0 1	19	2.0198	2.0244	3	2 7 3
23	5.75	5.8244	6	1 3 0			2.8488	3	6 2 0			2.0179	2	5 2 4
		5.6975	13	3 1 0			2.8310	3	2 5 2			1.9988	3	1 9 1
100	5.43	5.4321	68	2 2 1			2.8087	2	2 3 3			1.9941	2	7 2 3
		5.1536	9	3 0 1	23	2.806	2.7996	11	3 2 3			1.9807	3	8 4 1
33	5.07	5.0568	6	0 0 2			2.7923	2	5 2 2	22	1.9794	1.9759	3	0 2 5
		5.0473	18	1 3 1			2.7461	2	4 5 1			1.9733	3	2 0 5
9	4.920	4.9640	3	3 1 1	25	2.732	2.7421	11	6 2 1			1.9605	4	5 7 2
		4.8677	7	1 0 2			2.7160	7	4 4 2	18	1.9455	1.9457	2	7 5 2
25	4.618	4.6176	10	0 4 0			2.6921	2	1 4 3			1.9415	3	3 9 0
		4.5386	3	2 3 1	7	2.651	2.6452	3	5 3 2			1.9319	2	6 0 4
		4.5003	2	3 2 1			2.6295	3	0 6 2	12	1.9074	1.9067	2	3 9 1
13	4.488	4.4922	7	4 0 0			2.5394	3	4 6 0			1.9049	2	0 8 3
		4.4354	2	0 2 2	19	2.521	2.5278	5	1 7 1			1.8692	2	8 0 3
		4.4067	2	2 0 2			2.5236	5	2 6 2	14	1.8665	1.8678	2	7 4 3
9	4.301	4.3062	6	1 2 2			2.5037	2	1 0 4			1.8665	3	9 3 1
22	4.199	4.2005	19	0 4 1			2.4820	4	6 2 2			1.8635	2	2 8 3
37	4.104	4.1054	25	4 0 1	11	2.469	2.4658	2	7 1 1	8	1.8431	1.8471	3	0 10 0
		4.0902	6	1 4 1			2.4559	2	2 7 1			1.8433	2	6 3 4
34	3.984	3.9772	27	2 2 2			2.4372	4	5 1 3	13	1.8101	1.8146	2	2 4 5
		3.8639	8	3 0 2	3	2.436	2.4165	3	1 2 4			1.8087	2	4 2 5
15	3.827	3.8185	3	1 3 2	3	2.375	2.3760	4	5 2 3			1.7943	3	8 5 2
		3.8052	2	2 4 1			2.3285	4	4 4 3	18	1.7869	1.7928	2	7 1 4
		3.7820	5	3 1 2	8	2.318	2.3197	3	1 7 2			1.7890	3	2 7 4
11	3.591	3.6184	6	1 5 0			2.2889	3	7 0 2			1.7873	2	7 5 3
		3.5834	3	2 3 2			2.2716	3	7 1 2	11	1.7541	1.7530	3	0 9 3
		3.5645	4	3 2 2	15	2.265	2.2693	2	4 6 2			1.7512	2	4 9 2
		3.4099	5	0 4 2			2.2638	5	2 7 2	8	1.6889	1.6889	2	9 2 3
11	3.383	3.4069	2	1 5 1			2.2586	3	3 2 4			1.6844	2	4 10 1
		3.3584	8	4 0 2			2.2217	2	7 2 2			1.6750	2	2 8 4
		3.3501	3	1 4 2			2.2177	2	0 4 4	7	1.6658	1.6582	2	0 2 6
12	3.344	3.3308	3	5 1 1			2.2038	3	2 6 3			1.6567	2	2 0 6
		3.3164	3	0 1 3	12	2.190	2.1834	2	2 8 1	7	1.6126	1.6202	2	8 7 2
5	3.217	3.2199	6	4 4 0			2.1779	4	4 5 3			1.6030	2	7 9 0
7	3.161	3.1668	5	0 2 3			2.1531	2	2 4 4			1.5940	2	4 8 4
		3.1187	3	1 2 3	9	2.134	2.1432	3	4 2 4	16	1.5897	1.5921	2	9 7 0
		3.1037	5	5 3 0			2.1269	2	5 7 0			1.5909	2	5 5 5
11	3.086	3.0784	2	0 6 0			2.1080	5	7 5 0			1.5832	3	7 9 1
		3.0682	3	4 4 1	19	2.091	2.1003	2	0 8 2	9	1.5691	1.5728	2	9 7 1
		3.0024	6	3 5 1			2.0861	2	1 8 2	5	1.5477	1.5594	2	2 4 6
21	2.987	2.9948	4	6 0 0			2.0814	5	5 7 1			1.5556	2	4 2 6
		2.9867	4	2 2 3			2.0726	2	1 5 4	8	1.5217	1.5280	2	7 9 2
		2.9671	4	5 3 1								1.5186	2	9 7 2
										6	1.4999	1.5003	2	2 12 1
										7	1.4746	1.4779	3	11 5 1

https://doi.org/10.1180/minmag.2017.081.085 Published online by Cambridge University Press

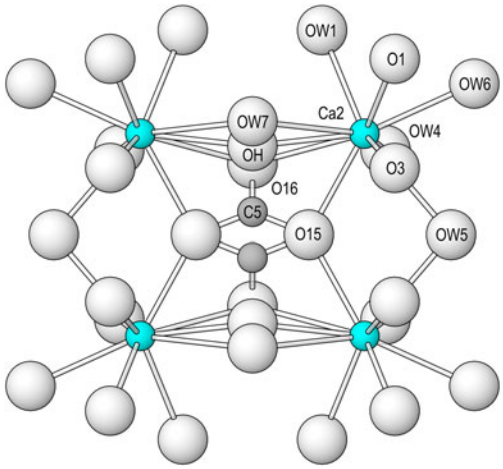

FIG. 4. The grouping of Ca2 polyhedra in markeyite, viewed down [001], showing the linkage by the partially occupied C5 carbonate group, OH and OW7.

and radiation noted above. The data were processed using the *Rigaku CrystalClear* software package and an empirical (multi-scan) absorption correction was applied using the *ABSCOR* program (Higashi, 2001) in the *CrystalClear* software suite. The structure was solved by direct methods using *SIR2011* (Burla *et al.*, 2012). *SHELXL-2013* (Sheldrick, 2015) was used for the refinement of the structure.

Determining the locations of most atoms was straightforward. The initial structure determination showed that the O15 site, nearly fully occupied by O, is only 2.28 Å from an equivalent O15 site. We first thought that the short O15–O15 distance could be indicative of a very strong hydrogen bond; however, the distance is typical for an O–O edge of a CO_3 group. Closer examination of difference-Fourier maps revealed that two partially-occupied CO_3 groups (centred by C5) share this O15–O15 edge and are completed by a partially occupied O site, O16. In subsequent refinements, the

TABLE 3. Data collection and structure refinement details for markeyite.*

Diffractometer	Rigaku R-Axis Rapid II
X-ray radiation/power	Mo$K\alpha$ (λ = 0.71075 Å)/50 kV, 40 mA
Temperature (K)	293(2)
Structural formula	$Ca_9(UO_2)_4(CO_3)_{12.71}(OH)_{0.50}\cdot 28.25H_2O$
Space group	*Pmmn*
Unit-cell dimensions	a = 17.9688(13) Å
	b = 18.4705(6) Å
	c = 10.1136(4) Å
V	3356.6(3) Å^3
Z	2
Density (for above formula)	2.692 g cm^{-3}
Absorption coefficient	10.45 mm^{-1}
F(000)	2561
Crystal size (μm)	110 × 80 × 10
θ range (°)	3.16 to 27.49
Index ranges	$-23 \le h \le 22$, $-23 \le k \le 22$, $-13 \le l \le 13$
Reflections collected/unique	22,867/4045; R_{int} = 0.062
Reflections with $F > 4\sigma F$	3427
Completeness to θ = 27.49°	98.8%
Max./min. transmission	0.903/0.393
Refinement method	Full-matrix least-squares on F^2
Restraints/parameters	3/280
GoF	1.054
Final R indices [$F > 4\sigma(F)$]	R_1 = 0.0435, wR_2 = 0.0987
R indices (all data)	R_1 = 0.0544, wR_2 = 0.1034
Largest diff. peak/hole ($e\cdot$A^{-3})	+3.60/–2.28

*$R_{int} = \Sigma|F_o^2 - F_o^2(\text{mean})|/\Sigma[F_o^2]$. GoF = $S = \{\Sigma[w(F_o^2 - F_c^2)^2]/(n-p)\}^{1/2}$. $R_1 = \Sigma||F_o| - |F_c||/\Sigma|F_o|$. $wR_2 = \{\Sigma[w(F_o^2 - F_c^2)^2]/\Sigma[w(F_o^2)^2]\}^{1/2}$; $w = 1/[\sigma^2(F_o^2) + (aP)^2 + bP]$ where a = 0.0420, b = 40.5434 and $P = [2F_c^2 + \text{Max}(F_o^2, 0)]/3$.

https://doi.org/10.1180/minmag.2017.081.085 Published online by Cambridge University Press

TABLE 4. Atom coordinates and displacement parameters (Å^2) for markeyite.

	x/a	*y/b*	*z/c*	U_{eq}	U^{11}	U^{22}	U^{33}	U^{23}	U^{13}	U^{12}
U1	0.47538(2)	0.75	0.98772(4)	0.02223(12)	0.0223(2)	0.0189(2)	0.0255(2)	0	−0.00475(16)	0
U2	0.25	0.46729(2)	0.07707(4)	0.02281(12)	0.01450(18)	0.0305(2)	0.0234(2)	−0.00413(16)	0	0
Ca1	0.44024(8)	0.43680(8)	0.87250(15)	0.0195(3)	0.0151(6)	0.0205(7)	0.0228(8)	0.0009(6)	−0.0009(5)	−0.0001(6)
Ca2	0.37570(10)	0.63955(10)	0.61086(18)	0.0346(4)	0.0363(9)	0.0376(10)	0.0298(9)	−0.0053(7)	−0.0032(7)	0.0061(8)
Ca3	0.25	0.25	0.6838(4)	0.0347(8)	0.0196(15)	0.0254(17)	0.059(3)	0	0	0
C1	0.4296(4)	0.6138(4)	0.8744(8)	0.0244(16)	0.027(4)	0.024(4)	0.023(4)	−0.002(3)	0.001(3)	−0.005(3)
C2	0.6094(4)	0.4956(4)	0.8050(8)	0.0240(16)	0.020(3)	0.031(4)	0.021(4)	0.004(3)	−0.004(3)	−0.003(3)
C3	0.25	0.4050(6)	0.8168(11)	0.025(2)	0.023(5)	0.032(6)	0.022(6)	−0.006(5)	0	0
C4	0.4235(6)	0.25	0.7923(12)	0.026(2)	0.024(5)	0.022(5)	0.034(6)	0	−0.010(5)	0
C5	0.25	0.7230(15)	0.576(3)	0.030(9)	0.027(18)	0.022(14)	0.04(2)	−0.012(13)	0	0
O1	0.4097(3)	0.5575(3)	0.8153(6)	0.0270(12)	0.032(3)	0.018(3)	0.031(3)	−0.002(2)	−0.007(2)	0.001(2)
O2	0.4704(3)	0.6158(3)	0.9798(5)	0.0286(13)	0.035(3)	0.023(3)	0.028(3)	0.002(2)	−0.013(2)	0.004(2)
O3	0.4096(3)	0.6771(3)	0.8283(6)	0.0336(14)	0.044(4)	0.020(3)	0.036(3)	−0.001(2)	−0.020(3)	0.000(3)
O4	0.5499(3)	0.4702(3)	0.7577(6)	0.0287(13)	0.017(3)	0.038(3)	0.030(3)	0.000(2)	−0.001(2)	−0.007(2)
O5	0.6721(3)	0.4931(4)	0.7421(6)	0.0371(15)	0.015(2)	0.071(4)	0.026(3)	−0.013(3)	0.004(2)	−0.005(3)
O6	0.3866(3)	0.4730(3)	0.0800(5)	0.0298(13)	0.020(3)	0.045(3)	0.025(3)	−0.008(3)	0.000(2)	0.002(3)
O7	0.25	0.3731(4)	0.7068(8)	0.0276(17)	0.026(4)	0.032(4)	0.024(4)	−0.008(3)	0	0
O8	0.3100(3)	0.4211(4)	0.8783(6)	0.0335(14)	0.018(3)	0.052(4)	0.030(3)	−0.015(3)	0.001(2)	−0.002(3)
O9	0.3792(4)	0.25	0.6935(9)	0.034(2)	0.026(4)	0.034(4)	0.043(5)	0	−0.016(4)	0
O10	0.4483(3)	0.3088(3)	0.8460(6)	0.0351(14)	0.040(3)	0.024(3)	0.042(4)	0.000(3)	−0.020(3)	0.001(3)
O11	0.3970(5)	0.75	0.0941(9)	0.038(2)	0.031(5)	0.035(5)	0.049(6)	0	−0.001(4)	0
O12	0.5540(5)	0.75	0.8808(10)	0.042(2)	0.036(5)	0.039(5)	0.050(6)	0	0.007(4)	0
O13	0.25	0.3777(5)	0.1403(9)	0.039(2)	0.033(5)	0.038(5)	0.044(5)	0.003(4)	0	0
O14	0.25	0.5564(5)	0.0134(9)	0.035(2)	0.030(4)	0.033(5)	0.042(5)	−0.001(4)	0	0
O15	0.3137(5)	0.75	0.5822(10)	0.045(4)	0.029(6)	0.058(8)	0.049(7)	0	−0.005(4)	0
O16	0.25	0.6690(18)	0.489(4)	0.082(16)	0.043(19)	0.08(3)	0.12(4)	−0.02(3)	0	0
OH	0.25	0.6531(18)	0.628(4)	0.037(13)	0.028(18)	0.024(18)	0.06(3)	−0.012(17)	0	0
OW1	0.3281(4)	0.5260(4)	0.5243(6)	0.0416(16)	0.047(4)	0.045(4)	0.033(3)	−0.008(3)	0.001(3)	0.005(3)
OW2	0.4080(3)	0.4127(3)	0.6367(6)	0.0330(14)	0.035(3)	0.039(3)	0.025(3)	−0.002(3)	−0.002(2)	−0.009(3)
OW3	0.25	0.6746(7)	0.2409(15)	0.084(4)	0.091(10)	0.052(7)	0.109(12)	−0.016(7)	0	0
OW4	0.3994(5)	0.6575(4)	0.3744(7)	0.0533(19)	0.075(5)	0.055(4)	0.030(4)	−0.009(3)	0.000(4)	0.013(4)
OW5	0.4729(7)	0.75	0.5764(15)	0.074(4)	0.057(7)	0.059(8)	0.105(11)	0	0.009(7)	0
OW6	0.4990(4)	0.5848(5)	0.5845(7)	0.061(2)	0.058(5)	0.077(6)	0.046(5)	0.026(4)	0.020(4)	0.030(4)
OW7	0.25	0.6261(7)	0.7475(13)	0.042(4)	0.033(6)	0.054(8)	0.040(8)	0.011(6)	0	0
OW8	0.25	0.75	0.9025(19)	0.067(5)	0.043(9)	0.068(11)	0.089(14)	0	0	0
OW9	0.25	0.25	0.9269(15)	0.063(5)	0.115(15)	0.032(7)	0.043(9)	0	0	0
OW10	0.6245(10)	0.6744(10)	0.6682(16)	0.120(9)	0.109(14)	0.158(17)	0.095(13)	0.008(11)	0.010(10)	0.026(12)
OW11	0.25	0.25	0.462(2)	0.075(11)	0.084(19)	0.10(3)	0.039(14)	0	0	0
OW12	0.25	0.174(3)	0.455(5)	0.09(2)						

* Occupancies: C5/O16: 0.35(3); O15: 0.93(4); OH/OW7: 0.25/0.75(3); OW10: 0.75(3); OW11/OW12: 0.71/0.29(5).

occupancies of the C5 and O16 sites were refined as equivalent. Another partially occupied O site (OH) was located 1.43 Å from the O16 site and 1.31 Å from OW7 on the opposite side. The OH site cannot be occupied when either the O16 or OW7 site is occupied. In subsequent refinements, the occupancies of the OW7 and OH sites were refined with a combined occupancy of 1.0. The aforementioned sites are shown in Fig. 4. There are three other partially occupied O sites, OW10, OW11 and OW12. The OW11 and OW12 sites are separated by only 1.41 Å; consequently, their occupancies were refined with a combined occupancy of 1.0. In the final refinement, soft distance restraints were placed on the distances between the atoms in the $C5O_3$ group, which slightly improved the refinement and bond-valence sums. All sites, except the low-occupancy OW12 site, were refined with anisotropic displacement parameters.

Data collection and refinement details are given in Table 3, atom coordinates and displacement parameters in Table 4, selected bond distances in Table 5 and a bond-valence analysis in Table 6. The crystallographic information files have been deposited with the Principal Editor of *Mineralogical Magazine* and are available as Supplementary material (see below).

Description and discussion of the structure

Two U sites (U1 and U2) in the structure of markeyite are each surrounded by eight O atoms forming a squat UO_8 hexagonal bipyramid. These bipyramids are each chelated by three CO_3 groups, forming uranyl tricarbonate clusters (UTC) of formula $[(UO_2)(CO_3)_3]^{4-}$ (Burns 2005; Fig. 5). There are three different Ca–O polyhedra in the

TABLE 5. Selected bond distances (Å) for markeyite.

Ca1–O8	2.360(5)	U1–O11	1.773(9)	U2–O14	1.768(9)
Ca1–O1	2.368(5)	U1–O12	1.779(9)	U2–O13	1.773(9)
Ca1–O4	2.369(6)	U1–O3(×2)	2.411(5)	U2–O5(×2)	2.416(6)
Ca1–O10	2.383(6)	U1–O10(×2)	2.427(6)	U2–O8(×2)	2.436(6)
Ca1–O2	2.399(5)	U1–O2(×2)	2.481(5)	U2–O6(×2)	2.457(5)
Ca1–O6	2.404(6)	<U1–O_{ap}>	1.776	<U2–O_{ap}>	1.771
Ca1–OW2	2.494(6)	<U1–O_{eq}>	2.440	<U2–O_{eq}>	2.436
<Ca1–O>	2.397				
		C1–O1	1.250(9)	Hydrogen bonds	
Ca2–OH	2.279(5)	C1–O2	1.295(9)	OW1···O5	2.717(9)
Ca2–O15	2.343(5)	C1–O3	1.309(9)	OW1···OH	2.93(3)
Ca2–O3	2.384(6)	<C1–O>	1.285	OW2···O7	3.017(6)
Ca2–OW1	2.428(7)			OW2···O9	3.103(6)
Ca2–OW6	2.450(7)	C2–O4	1.261(9)	OW3···O11	3.334(12)
Ca2–OW4	2.451(7)	C2–O5	1.296(9)	OW4···O4	2.859(9)
Ca2–O16	2.63(2)	C2–O6	1.301(9)	OW6···O1	2.876(9)
Ca2–O1	2.635(6)	<C2–O>	1.286	OW6···O4	2.896(9)
Ca2–OW7	2.660(7)			OW7···O14	2.981(16)
Ca2–OW5	2.708(8)	C3–O7	1.258(13)	OW8···O11	3.276(15)
<Ca2–O>*	2.503	C3–O8(×2)	1.279(8)	OW9···O13	3.197(17)
		<C3–O>	1.272	OW10···O12	2.861(19)
Ca3–OW11(×2)	2.24(3)			OW10···O13	3.124(18)
Ca3–O7(×2)	2.286(8)	C4–O9	1.278(13)		
Ca3–O9(×2)	2.324(8)	C4–O10(×2)	1.294(8)	Hydrogen bonds to H_2O groups are not included.	
Ca3–OW9	2.459(16)	<C4–O>	1.289		
Ca3–OW12(×2)	2.71(6)				
<Ca3–O>*	2.347	C5–O15(×2)	1.250(13)		
		C5–O16	1.33(2)		
		<C5–O>	1.277		

* Weighted average based on partial occupancies of OH, O15, O16, OW7, OW11 and OW12 sites; the effective coordination of Ca2 is 8.27 and that of Ca3 is 7.00.

https://doi.org/10.1180/minmag.2017.081.085 Published online by Cambridge University Press

TABLE 6. Bond-valence analysis for markeyite. Values are expressed in valence units.*

	Ca1	Ca2	Ca3	U1	U2	C1	C2	C3	C4	C5	Hydrogen bonds	Sum
O1	0.32	0.15				1.46					0.16	2.09
O2	0.29			0.44 × 2↓		1.29						2.02
O3		0.30		0.50 × 2↓		1.24						2.04
O4	0.32						1.42				0.16, 0.15	2.05
O5					0.49 × 2↓		1.29				0.22	2.00
O6	0.29				0.46 × 2↓		1.27					2.02
O7			0.40 × 2↓					1.43			0.13	1.96
O8	0.33				0.48 × 2↓			1.35 × 2↓				2.16
O9			0.36 × 2↓						1.36		0.11, 0.11	1.94
O10	0.30			0.48 × 2↓					1.30 × 2↓			2.08
O11				1.71							0.09, 0.09, 0.09	1.98
O12				1.69							0.16	1.85
O13					1.71						0.11, 0.10	1.92
O14					1.73						0.13	1.86
O15		0.34 × 0.93↓			0.49					1.46		2.29
O16		0.15 × 0.34↓			0.49					1.18		1.82
OH		0.41 × 2→, ×0.25↓									0.15, 0.15	1.12
OW1		0.27										
OW2	0.22											
OW3												
OW4		0.25									Hydrogen bond	
OW5		0.12									contributions	
OW6		0.25									to OW sites and	
OW7		0.14 × 0.75↓									bond-valence sums	
OW8											for OW sites are	
OW9			0.25								not included.	
OW10												
OW11			0.46 × 0.71↓									
OW12			0.12 × 0.58↓									
Sum	2.07	1.92	2.17	6.24	6.29	4.00	3.98	4.13	3.95	4.10		

* Multiplicity is indicated by ×↓→. Bond strength contributions to Ca sites from partially occupied O sites are adjusted for their occupancies. Ca^{2+}–O and C^{4+}–O bond-valence parameters from Brown and Altermatt (1985); U^{6+}–O bond valence parameters from Burns *et al*. (1997); hydrogen-bond strengths based on O–O bond lengths from Ferraris and Ivaldi (1988).

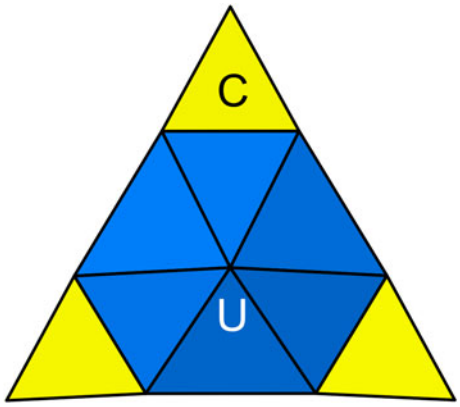

FIG. 5. The uranyl tricarbonate cluster (UTC) of formula $[(UO_2)(CO_3)_3]^{4-}$.

structure: Ca1 bonds to seven fully occupied O sites; Ca2 bonds to five fully occupied and five partially occupied O sites (Fig. 4) for a total effective coordination of 8.27; and Ca3 bonds to five fully occupied and four partially occupied O sites for a total effective coordination of 7. The three Ca–O polyhedra share edges and corners with the UTCs in very different ways. The Ca1 polyhedra share edges with U1 and U2 bipyramids and corners with C1 and C2 triangles in different UTCs. Pairs of Ca2 polyhedra share an edge to form a dimer, which is linked to a second dimer through the partially occupied C5 triangles and OH and OW7 sites. The group of four Ca2 polyhedra (and C5 triangle) is linked to two U1 UTCs by edge sharing between Ca2 polyhedra and C1 triangles. The Ca3 polyhedra share corners with two C3 and two C4 triangles, each being in a different UTC. The linkages between UTCs and Ca polyhedra form thick corrugated heteropolyhedral layers parallel to {010} (Fig. 5) and these layers link to one another and to interlayer H_2O groups (OW3, OW8 and OW10) only via hydrogen bonds (Fig. 6).

The formula based upon the refined structure is $Ca_9(UO_2)_4(CO_3)_{12.71}(OH)_{0.50}\cdot 28.25H_2O$. The ideal formula assumes full occupancy of the O15 site and half occupancy of the C5 and O16 sites, providing one CO_3 group per formula unit. The OH site, with an occupancy of 0.25, is combined with the nearby OW7 site, with a refined occupancy of 0.75. The resultant ideal formula is $Ca_9(UO_2)_4(CO_3)_{13}\cdot 28H_2O$.

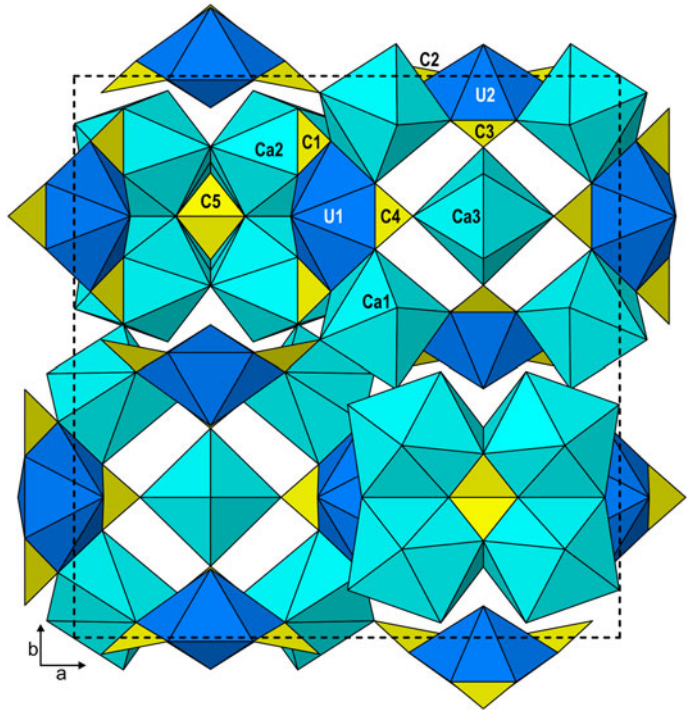

FIG. 6. The heteropolyhedral layer in markeyite.

https://doi.org/10.1180/minmag.2017.081.085 Published online by Cambridge University Press

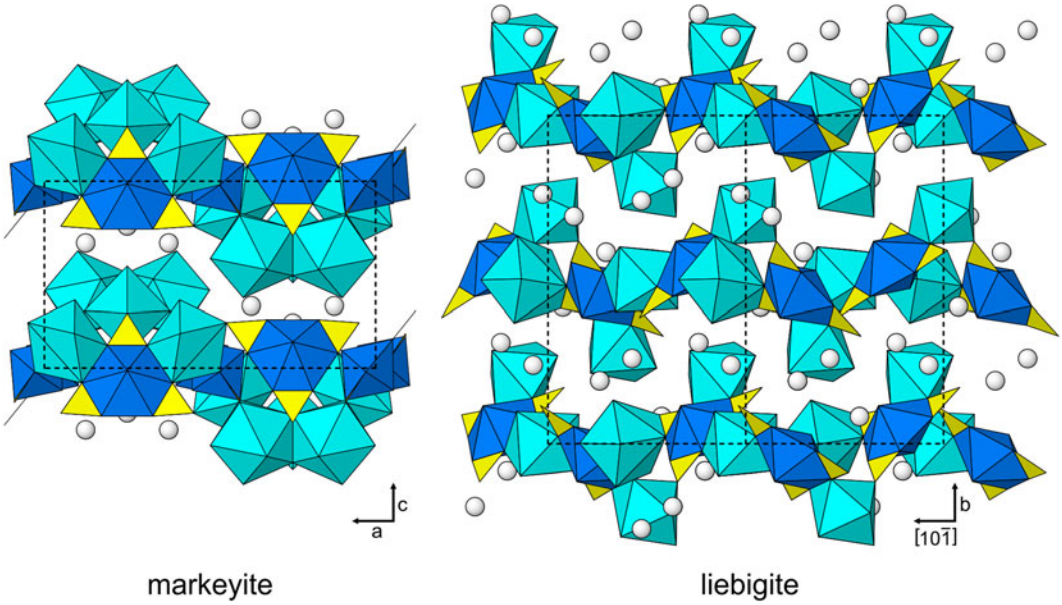

FIG. 7. The structures of markeyite and liebigite viewed parallel to the heteropolyhedral layers. UO_8 hexagonal bipyramids are dark blue, CO_3 triangles are yellow and Ca–O polyhedra are light blue; O atoms of isolated H_2O groups are white balls. Unit cell outlines are shown as dashed black lines.

The structure of liebigite, $Ca_2(UO_2)(CO_3)_3 \cdot 11H_2O$ (Mereiter, 1982), contains the same structural components as that of markeyite. The same types of polyhedral linkages occur in both structures. As in the structure of markeyite, the Ca–O polyhedra link the UTCs in the structure of liebigite forming thick corrugated heteropolyhedral layers and these layers link to one another and to interlayer H_2O groups only via hydrogen bonds (Fig. 7). However, topologies of the two structures are quite different. Of particular note, in the liebigite structure, one of the Ca–O polyhedra shares an edge with a CO_3 group of the UTC, but there is no such linkage in the markeyite structure.

Acknowledgements

Igor Pekov and an anonymous reviewer are thanked for their constructive comments on the manuscript. An anonymous CNMNC member is thanked for pointing out the likelihood that the short O15–O15 distance corresponds to the edge of an additional CO_3 group. A portion of this study was funded by the John Jago Trelawney Endowment to the Mineral Sciences Department of the Natural History Museum of Los Angeles County. This research was also financially supported by GACR post-doctoral Grant no. 13-31276P to J.P. and by the long-term project DKRVO 2016-02 of the Ministry of Culture of the Czech Republic (National Museum 00023272) to J.Č.

Supplementary material

To view supplementary material for this article, please visit https://doi.org/10.1180/minmag.2017.081.085

References

Anderson, A., Chieh, Ch., Irish, D.E. and Tong, J.P.K. (1980) An X-ray crystallographic, Raman, and infrared spectral study of crystalline potassium uranyl carbonate, $K_4UO_2(CO_3)_3$. *Canadian Journal of Chemistry*, **58**, 1651–1658.

Bartlett, J.R. and Cooney, R.P. (1989) On the determination of uranium-oxygen bond lengths in dioxouranium(VI) compounds by Raman spectroscopy. *Journal of Molecular Structure*, **193**, 295–300.

Brown, I.D. and Altermatt, D. (1985) Bond-valence parameters from a systematic analysis of the inorganic crystal structure database. *Acta Crystallographica*, **B41**, 244–247.

Burla, M.C., Caliandro, R., Camalli, M., Carrozzini, B., Cascarano, G.L., Giacovazzo, C., Mallamo, M.,

Mazzone, A., Polidori, G. and Spagna, R. (2012) *SIR*2011: a new package for crystal structure determination and refinement. *Journal of Applied Crystallography*, **45**, 357–361.

Burns, P.C. (2005) U^{6+} minerals and inorganic compounds: insights into an expanded structural hierarchy of crystal structures. *Canadian Mineralogist*, **43**, 1839–1894.

Burns, P.C., Ewing, R.C. and Hawthorne, F.C. (1997) The crystal chemistry of hexavalent uranium: polyhedron geometries, bond-valence parameters, and polymerization of polyhedra. *Canadian Mineralogist*, **35**, 1551–1570.

Čejka, J. (1999) Infrared spectroscopy and thermal analysis of the uranyl minerals. Pp. 521–622. in: *Uranium: Mineralogy, Geochemistry and the Environment* (P.C. Burns and R.C. Finch, editors). Reviews in Mineralogy, **38**. Mineralogical Society of America, Washington, DC.

Čejka, J. (2005) Vibrational spectroscopy of the uranyl minerals – infrared and Raman spectra of the uranyl minerals. II. Uranyl carbonates. *Bulletin mineralogicko-petrologického oddělení Národního muzea* (Praha), **13**, 62–72 [in Czech].

Chenoweth, W.L. (1993) *The Geology and Production History of the Uranium Deposits in the White Canyon Mining District, San Juan County, Utah*. Utah Geological Survey Miscellaneous Publication, **93–3**.

Ferraris, G. and Ivaldi, G. (1988) Bond valence vs. bond length in O···O hydrogen bonds. *Acta Crystallographica*, **B44**, 341–344.

Hålenius, U., Hatert, F., Pasero, M. and Mills, S.J. (2017) New minerals and nomenclature modifications approved in 2017. *CNMNC Newsletter No.* 38, August 2017, page 1038; *Mineralogical Magazine*, **81**, 1033–1038.

Higashi, T. (2001) *ABSCOR*. Rigaku Corporation, Tokyo.

Kampf, A.R., Plášil, J., Kasatkin, A.V., Marty, J. and Čejka, J. (2016) Klaprothite, péligotite and ottohahnite, three new sodium uranyl sulfate minerals with bidentate UO_7–SO_4 linkages from the Blue Lizard mine, San Juan County, Utah, USA. *Mineralogical Magazine*, **80**, 753–779.

Kampf, A.R., Plášil, J., Kasatkin, A.V., Marty, J. and Čejka, J. (2017) Markeyite, IMA 2016-090. *CNMNC Newsletter No.* 35, February 2017, page 211; *Mineralogical Magazine*, **81**, 209–213.

Koglin, E., Schenk, H.J. and Schwochau, K. (1979) Vibrational and low temperature optical spectra of the uranyl tricarbonato complex $[UO_2(CO_3)_3]^{4-}$. *Spectrochimica Acta*, **35A**, 641–647.

Libowitzky, E. (1999) Correlation of O–H stretching frequencies and O–H···O hydrogen bond lengths in minerals. *Monatshefte für Chemie*, **130**, 1047–1059.

Mandarino, J.A. (1976) The Gladstone-Dale relationship – Part 1: derivation of new constants. *Canadian Mineralogist*, **14**, 498–502.

Mandarino, J.A. (2007) The Gladstone–Dale compatibility of minerals and its use in selecting mineral species for further study. *Canadian Mineralogist*, **45**, 1307–1324.

Mereiter, K. (1982) The crystal structure of liebigite, $Ca_2UO_2(CO_3)_3\cdot\sim 11H_2O$. *Tschermaks Mineralogische und Petrographische Mitteilungen*, **30**, 277–288.

Olds, T.A., Sadergaski, L., Plášil, J., Kampf, A.R., Burns, P.C., Steele, I.M. and Marty, J. (2016) Leoszilardite, IMA 2015-128. *CNMNC Newsletter No.* 31, June 2016, page 694; *Mineralogical Magazine*, **80**, 691–697.

Sheldrick, G.M. (2015) Crystal structure refinement with *SHELX*. *Acta Crystallographica*, **C71**, 3–8.

https://doi.org/10.1180/minmag.2017.081.085 Published online by Cambridge University Press